

Letter

Amino acid conjugation of oxIAA is a secondary metabolic regulation involved in auxin homeostasis

Dynamic regulation of the concentration of the natural auxin indole-3-acetic acid (IAA) is essential to coordinate most physiological and developmental processes and responses to environmental changes (reviewed in Friml, 2022). Auxin inactivation plays a crucial role in auxin homeostasis and metabolism. The primary enzymes involved in auxin metabolism have been known for some time. Members of the acyl acid amide synthetases belonging to the GRETCHEN HAGEN 3 (GH3) and the amidohydrolase IAA-LEUCINE RESISTANT 1 (ILR1) and ILR1-like (ILL) families catalyze the conjugation of IAA to amino acids and hydrolysis of the IAA-amino acid conjugates, respectively (LeClere *et al.*, 2002; Staswick *et al.*, 2005). The DIOXIGENASE FOR AUXIN OXIDATION (DAO) enzymes were shown to catalyze the oxidation of IAA to form oxIAA (Porco *et al.*, 2016; Zhang *et al.*, 2016). Albeit these IAA-inactivating enzymes appeared to participate in different catabolic routes, very recently, it was reported that GH3, ILR1, and DAO are part of a single linear pathway rather than two distinct ways (Hayashi *et al.*, 2021). According to this model, IAA is mainly inactivated by GH3 enzymes, DAO functions as an oxidase of IAA-amino acid conjugates to produce oxIAA-amino acid conjugates downstream of GH3, and oxIAA is produced from oxIAA-amino acid hydrolysis by ILR1. Therefore, DAO and ILR1 enzymes appeared to play a role in this pathway that differs from that assigned initially. Although GH3 enzymes are known to possess catalytic promiscuity accepting various substrates and amino acids, a possible additional role of GH3s in auxin inactivation was not investigated (Staswick *et al.*, 2005; Westfall *et al.*, 2012). Besides, while the new model proposed by Hayashi *et al.* (2021) was described to occur in angiosperms, whether it operates in nonflowering species remains unknown (Ross & Gélinas-Marion, 2021). GRETCHEN HAGEN 3 proteins are highly conserved all over the plant kingdom, whereas DAO and DAO-like enzymes have specifically evolved with angiosperms (Okrent & Wildermurth, 2011; Brunoni *et al.*, 2020; Kaneko *et al.*, 2020; Takehara *et al.*, 2020). Here, we report the evidence of oxIAA-amino acid conjugation being catalyzed by the group of IAA-conjugating enzymes belonging to the Group II of GH3s. Our work suggests that the contribution of this pathway to auxin homeostasis is species-dependent.

Materials and Methods

Plant material and growth conditions

Arabidopsis thaliana (L.) Heynh. seeds wild-type (WT) Col-0 and *gh3* sextuple mutant (*gh3.1*, *gh3.2*, *gh3.3*, *gh3.4*, *gh3.5*, and *gh3.6*; Porco *et al.*, 2016) were gas sterilized with chlorine gas (10 ml of HCl (35%) in 50 ml of bleach) for at least 2 h in an airtight box. Seeds were then sown under sterile conditions on Petri dishes containing ½ Murashige-Skoog (½MS) medium (2.15 g salts including vitamins per 1 l) with 1% sucrose and 0.5 g l⁻¹ MES monohydrate at pH 5.7 and solidified with 0.57% Gellan gum. Stratification was carried out for 3 d at 4°C, and then, plates were transferred to light at 22 ± 1°C, under long-day (LD) conditions (16 h : 8 h, light : dark photoperiod; 100 μmol m⁻² s⁻¹). Gametophores from *Physcomitrium patens* (Hedw.) Mitt. Wild-type and knockout lines (International Moss Stock Center IMSC#40207 GH3-1/B34, IMSC#40208 GH3-2/22, and IMSC#40209 GH3-doKO-A96; Bierfreund *et al.*, 2004; Ludwig-Müller *et al.*, 2009) were obtained from IMSC (www.moss-stock-center.org) and cultured axenically in Knop medium (100 mg l⁻¹ Ca(NO₃)₂·4H₂O, 25 mg l⁻¹ KCl, 25 mg l⁻¹ KH₂PO₄, 25 mg l⁻¹ MgSO₄·7H₂O, and 1.25 mg l⁻¹ FeSO₄·7H₂O, pH 5.8) including 92.05 mg l⁻¹ ammonium tartrate, 0.5 mg l⁻¹ nicotinic acid, 0.125 mg l⁻¹ *p*-amino benzoic acid, 2.5 mg l⁻¹ thiamine HCl, trace-element solution (0.614 mg l⁻¹ H₃BO₃, 0.389 mg l⁻¹ MnCl₂·4H₂O, 0.059 mg l⁻¹ NiCl₂·6H₂O, 0.055 mg l⁻¹ CoCl₂·6H₂O, 0.055 mg l⁻¹ CuSO₄·5H₂O, 0.055 mg l⁻¹ ZnSO₄·7H₂O, 0.0386 mg l⁻¹ Al₂(SO₄)₃·18H₂O, 0.028 mg l⁻¹ KBr, 0.028 mg l⁻¹ KI, 0.028 mg l⁻¹ LiCl, and 0.028 mg l⁻¹ SnCl₂·2H₂O), and 200 mg l⁻¹ glucose. The medium was solidified with 1.5% plant agar. Plants were cultured in a growth chamber at 22 ± 1°C, under LD conditions, and subcultured onto fresh medium every 3 wk. *Picea abies* (L. Karst) seeds were provided by SkogForsk (Sävar, Sweden). Seeds were soaked in tap water for 12 h at 4°C and sown in fine wet vermiculite. Germination and seedling growth occurred in a growth chamber at 24°C during the day and 18°C at night, under LD conditions at a light intensity of 100 μmol m⁻² s⁻¹.

Feeding experiments and auxin metabolite profiling

Seven-day-after-germination (DAG), *A. thaliana* seedlings were transferred to sterile liquid ½MS medium for 24 h and subsequently supplemented with 50 μM IAA, IAA-Asp, IAA-Glu, or oxIAA for 6 and 24 h. Three-week-old moss gametophores were transferred to sterile liquid Knop medium for 24 h and subsequently supplemented with 50 μM IAA, IAA-Glu, or oxIAA for 24 h. Two-week-old spruce seedlings were transferred to ½MS liquid medium for 24 h and subsequently supplemented with 50 μM IAA, IAA-Asp, IAA-Glu, or oxIAA for 6 h; for the inhibition of oxIAA conjugation in spruce, 2-wk-old seedlings were

incubated in 1/2MS liquid medium with 50 μ M kakeimide (KKI), 5 μ M oxIAA, or a combination of 50 μ M KKI and 5 μ M oxIAA for 6 h. Mock-treated Arabidopsis, moss, and spruce plants were used as control. All liquid cultures were kept under gentle shaking and in darkness for the whole experiment in a growth chamber at 24°C during the day and 18°C during the night. For each time point, *A. thaliana* whole seedlings, *P. patens* gametophores, and *P. abies* roots were collected in three replicates (10 mg tissue per sample). Sample purification and quantification of oxIAA–Asp and oxIAA–Glu were performed as described previously (Pěncík *et al.*, 2018). Briefly, samples were extracted with 1 ml of 50 mM sodium phosphate buffer, pH 7.0, containing 0.1% sodium diethyldithiocarbamate. oxIAA–[¹³C₄, ¹⁵N]Asp and oxIAA–[¹³C₅, ¹⁵N]Glu were added as internal standards. Two hundred microliters of the extract was acidified with 1 M HCl to pH 2.7 and purified by in-tip micro solid phase extraction (in-tip μ SPE). After evaporation under reduced pressure, samples were analyzed using HPLC system 1260 Infinity II (Agilent Technologies, Santa Clara, CA, USA) equipped with Kinetex C18 column (50 mm \times 2.1 mm, 1.7 μ m; Phenomenex, Torrance, CA, USA) and linked to 6495 Triple Quad detector (Agilent Technologies).

Cloning, protein production, and bacterial enzyme assay

Cloning and protein production of AtGH3s (AtGH3.1–5, 7–16, 18, 19) and PpGH3s (PpGH3.1 and PpGH3.2) were performed as described previously (Brunoni *et al.*, 2020). Primers used for cloning are listed in Supporting Information Table S1. *Escherichia coli* BL21 (DE3) strains expressing recombinant AtGH3.6, AtGH3.17, and PaGH3s (PaGH3.16, PaGH3.17, PaGH3.gII.8, and PaGH3.gII.9) used in this work were previously generated (Brunoni *et al.*, 2019, 2020). Briefly, the production of recombinant proteins was induced by adding 0.1 mM isopropyl- β -D-thiogalactopyranoside (IPTG) to cell cultures in a liquid medium with OD₆₀₀ between 0.6 and 0.8. Cells were grown overnight at 20°C with constant shaking at 180 rpm. Protein expression was tested by Western blotting with anti-6x His antibody horseradish peroxidase (HPR) conjugate. Fifty milliliters of GH3-producing bacteria were pelleted and resuspended in an equal volume of 1 \times phosphate-buffered saline (PBS) buffer. The crude cell lysate was obtained by sonication and clarified by centrifugation (21 325 g at 4°C for 30 min). Five hundred microliters of clarified cell lysate were incubated with 1 mM amino acid mixture, 3 mM ATP, 3 mM MgCl₂, and 1 mM auxin substrate (IAA or oxIAA) for 5 h at 30°C with constant shaking at 50 rpm in darkness. Sample preparation and quantification of IAA- and oxIAA-amino acid conjugates were performed as described previously (Brunoni *et al.*, 2020), using [¹³C₆]IAA–Asp, [¹³C₆]IAA–Glu, oxIAA–[¹³C₄, ¹⁵N]Asp, and oxIAA–[¹³C₅, ¹⁵N]Glu as internal standards.

Protein purification and enzyme kinetics of AtGH3.2 and AtGH3.6

Two hundred milliliters of overnight-induced AtGH3.2- and AtGH3.6-producing bacterial cultures were used for protein purification. Cell lysis and protein extraction were done using the cell lyser

One Shot model (Constant Systems Ltd, Northamptonshire, UK) at 24 000 psi in the presence of cComplete EDTA-free Protease Inhibitor Cocktail (Roche), followed by treatment with DENARASE (c-LEcta GmbH, Leipzig, Germany). Recombinant AtGH3.2 and AtGH3.6 were purified on a Nickel-HiTrap IMAC FF column (Cytiva Life Sciences, Marlborough, MA, USA) on an NGC Medium-Pressure Liquid Chromatography System into 50 mM Tris–HCl buffer, pH 7.4, 300 mM NaCl, and 5% glycerol. The yield after purification was about 14.4 mg for GH3.2 and 2.4 mg for GH3.6, respectively, per 200 ml of *E. coli* BL21 (DE3) cells. The enzyme activity and saturation curves were measured in 50 mM Tris–HCl buffer, pH 8.0, 0.1 mM DTT, 30 mM ATP, 30 mM L-aspartic acid, 3 mM MgCl₂, and varying concentrations (0.1–8 mM) of auxin substrate (IAA or oxIAA). The reactions were carried out in triplicates at 30°C in the presence of 5 μ M enzyme for 30 min in darkness and stopped after adding 100% methanol. Sample preparation and quantification of oxIAA-amino acid conjugates were performed as described previously (Brunoni *et al.*, 2020), using [¹³C₆]IAA–Asp, [¹³C₆]IAA–Glu, oxIAA–[¹³C₄, ¹⁵N]Asp, and oxIAA–[¹³C₅, ¹⁵N]Glu as internal standards. Kinetic constants K_m and V_{max} were determined using the GraphPad PRISM 8.0 software (www.graphpad.com).

Statistical analysis

Statistical analysis was carried out using Microsoft Excel 2016 for Windows PC. Quantitative values are presented as mean \pm SD.

Arabidopsis Group II GH3 enzymes catalyze the conjugation of oxIAA to amino acids *in vitro* and *in planta*

We studied the oxIAA-conjugating activity of recombinant Arabidopsis GH3 enzymes after their production in *E. coli* to test a possible further involvement of GH3 enzymes in IAA inactivation, using a bacterial assay that was previously adopted to study the activity of several IAA catabolic enzymes (Brunoni *et al.*, 2019; Müller *et al.*, 2021). Arabidopsis possesses 19 different GH3 proteins classified into three groups (I, II, and III) based on substrate specificity and sequence homology (Staswick *et al.*, 2005). Group I GH3s conjugate jasmonic acid with isoleucine (Staswick & Tiryaki, 2004; Delfin *et al.*, 2022); Group II GH3s contain enzymes that conjugate auxins (Staswick *et al.*, 2005); and Group III, specific for *Brassicaceae*, contains proteins predicted to be active on benzoates (Okrent *et al.*, 2009; Holland *et al.*, 2019; Torrens-Spence *et al.*, 2019). While none of the members of Group I and III GH3s could accept oxIAA as a substrate for conjugation with amino acids, members of the Group II GH3s were able to catalyze the conversion of oxIAA (Dataset S1; Fig. S1). Among Group II, AtGH3.1, AtGH3.2, AtGH3.3, AtGH3.5, AtGH3.6, and AtGH3.17 showed activity with oxIAA (Fig. S1). By contrast, two members, namely AtGH3.4 and AtGH3.9, did not show any activity with this substrate (Dataset S1). AtGH3.2, AtGH3.3, and AtGH3.5 conjugated oxIAA with aspartate (Asp) preferentially, whereas AtGH3.1 and AtGH3.6 conjugated oxIAA exclusively with Asp and AtGH3.17 with glutamate (Glu; Fig. S1). Notably,

AtGH3.2 conjugates oxIAA also with leucine (Leu) and phenylalanine (Phe; Dataset S1). To assess the substrate specificity of Group II GH3 enzymes, we studied the enzymatic activity of recombinant AtGH3 enzymes *in vitro*. Our kinetic data with recombinant AtGH3.2 and AtGH3.6 revealed that both enzymes preferred IAA to oxIAA as a substrate for the conjugation with Asp (Dataset S2; Fig. 1a). AtGH3.6 displayed higher specific activity than AtGH3.2, and K_m values for auxin substrates are in low mM range (Dataset S2; Fig. 1b). Calculated catalytic efficiency (V_{max}/K_m) values showed that conjugation of oxIAA with Asp reached only 2% of that measured with IAA (Dataset S2; Fig. 1b). To investigate whether oxIAA conjugation occurred *in planta*, we carried out a feeding experiment by incubating WT Col-0 seedlings with oxIAA and sampled after 6 and 24 h (Dataset S2; Fig. 2a). For comparison, we also treated plants with IAA, IAA-Asp, and IAA-Glu (Dataset S2; Fig. 2a). Feeding experiments confirmed that the production of oxIAA-Asp and oxIAA-Glu mainly resulted from the oxidation of IAA-Asp and IAA-Glu, respectively, as described previously (Hayashi *et al.*, 2021), as a high level of oxIAA-Asp and oxIAA-Glu was detected after exogenous application of IAA-Asp and IAA-Glu, respectively (Dataset S2; Fig. 2a). Nonetheless, oxIAA-Asp and oxIAA-Glu also accumulated after feeding with oxIAA, suggesting that, although to a minor extent, oxIAA-amino acid conjugates originated from oxIAA conjugation (Dataset S2; Fig. 2a). To investigate whether the GH3 pathway is involved in oxIAA conjugation, we fed *gh3* sextuple mutant with oxIAA (Dataset S2; Fig. 1b). We observed a dramatic drop in oxIAA-Asp level when compared to WT (Dataset S2; Fig. 2b) after treatment with oxIAA, confirming that oxIAA conjugation with Asp is mediated by Group II GH3s. On the contrary, oxIAA-Glu levels were unaltered in WT and *gh3* sextuple mutant after feeding with oxIAA, most likely due to remaining GH3.17 activity (Porco *et al.*, 2016; Dataset S2; Fig. S2b). These results, together with previous findings (Hayashi *et al.*, 2021; Müller *et al.*, 2021), suggest that conjugation/oxidation/hydrolysis reactions play multiple roles in the IAA inactivation pathway to fine-tune auxin and auxin metabolite levels (Fig. 1c).

The contribution of oxIAA-amino acid conjugation to auxin inactivation is species-dependent

The Group II of the GH3 family emerged very early during the land plant evolution (Ludwig-Müller *et al.*, 2009; Okrent & Wildermurth, 2011; Brunoni *et al.*, 2020). Intrigued by the evidence collected with Arabidopsis, we undertook a similar experimental approach to elucidate these pathways in evolutionarily distant species. We chose the moss *P. patens* as a model for bryophytes and the conifer *Picea abies* as a model for gymnosperms, as these species were used in previous studies to investigate the evolutionary patterns in the auxin metabolism (Ludwig-Müller *et al.*, 2009; Brunoni *et al.*, 2020). *Physcomitrium patens* possesses only two GH3 enzymes (Ludwig-Müller *et al.*, 2009). In our experimental conditions, recombinant PpGH3.2, but not PpGH3.1, catalyzed the conjugation of oxIAA exclusively with Glu (Dataset S1; Fig. S3). A feeding experiment of moss WT gametophores with IAA, IAA-Glu, and oxIAA revealed

that oxIAA-Glu mainly originated from oxidation of IAA-Glu (Dataset S2; Fig. 2c). Nevertheless, oxIAA-Glu also accumulated after feeding with oxIAA (Fig. 2d). Results from the feeding of moss *gh3* knockout mutants with oxIAA confirmed that PpGH3.2 catalyzes the conjugation of oxIAA *in vivo*, as oxIAA conjugation was impaired in the *gh3.2* single knockout and *gh3.1 gh3.2* double knockout mutants (Dataset S2; Fig. 2d). The conifer *P. abies* possesses several GH3 proteins that fall within the Group II, and we previously characterized four members conjugating IAA (Brunoni *et al.*, 2020). We tested the ability of these recombinant PaGH3s to target oxIAA, and PaGH3.gII.8 and PaGH3.17 were observed to conjugate oxIAA (Dataset S1; Fig. S4). PaGH3.gII.8 conjugated oxIAA exclusively with Asp while PaGH3.17 preferred Glu but also Leu (Dataset S1; Fig. S4). Feeding spruce seedlings with IAA, IAA-Asp, IAA-Glu, and oxIAA showed that oxIAA-Asp and oxIAA-Glu accumulated predominantly after oxIAA treatment (Dataset S2; Fig. 2e,f) and to a minor extent after feeding with IAA-Asp and IAA-Glu, respectively (Dataset S2; Fig. 2e). As spruce mutant lines are unavailable, we chemically inhibited the GH3-catalyzed conjugation step with the GH3 inhibitor kakeimide (KKI; Hayashi *et al.*, 2021; Fukui *et al.*, 2022). KKI was demonstrated to inhibit the synthesis of IAA-amino acid conjugates by binding to the IAA binding site of the GH3-ATP complex to form a ternary complex, which is described to selectively target IAA-conjugating GH3s (Fukui *et al.*, 2022). Brunoni *et al.* (2020) previously reported that members of the spruce Group II GH3s showed IAA-conjugating activity. This evidence suggested that KKI could inhibit Group II GH3 conjugating activity in spruce seedlings. Co-treatment with oxIAA and KKI of spruce seedlings blocked the formation of oxIAA-Asp and oxIAA-Glu (Dataset S2; Fig. 2f), confirming that oxIAA conjugation is mediated by GH3 enzymes. Our results suggest that, in moss, the oxidative pathway is the main contributor to the formation of the oxIAA-amino acid conjugates, whereas the conjugation of oxIAA to amino acids contributes the least. On the contrary, our findings on spruce confirm that diversification of the homeostatic control of IAA occurred in conifers, as conjugation is the favored mechanism for oxIAA-amino acid conjugate formation. At the same time, the oxidation of IAA-amino acid conjugates is a minor metabolic route.

Conclusions

Many decades of research were required to identify the critical genes involved in auxin inactivation. Nonetheless, the mechanisms by which auxin-inactivating enzymes governed auxin metabolism remained fragmented, and these enzymes appear to participate in different catabolic pathways. Recent research discoveries placed the IAA-inactivating enzymes GH3, ILR1, and DAO into a single catabolic route and described it to occur in angiosperms (Hayashi *et al.*, 2021). Here, we undertook a functional analysis of GH3 enzymes and *in planta*-feeding assays using auxin catabolic intermediates in different genetic backgrounds or upon chemical knockdown of the auxin inactivation pathway to further study the mechanisms regulating IAA homeostasis in the distantly related species, Arabidopsis, *P. abies*, and *P. patens*. Our results suggest

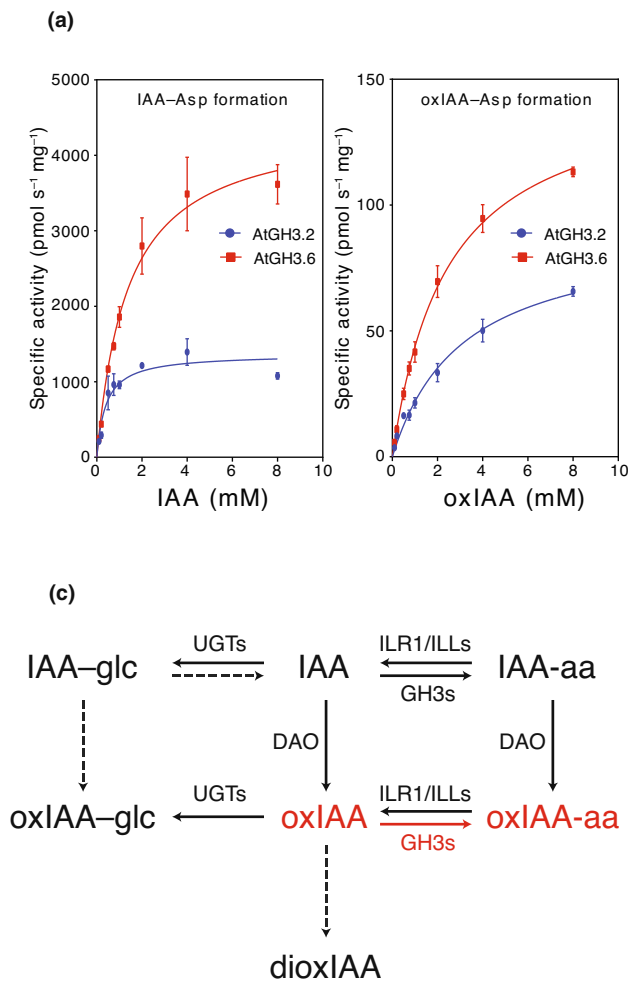


Fig. 1 Arabidopsis GRETCHEN HAGEN 3 (GH3) enzymes conjugate oxIAA with Asp *in vitro*. (a) Michaelis–Menten plots of the AtGH3.2 and AtGH3.6 enzymes for indole-3-acetic acid (IAA)–Asp (left panel) and oxIAA–Asp (right panel). (b) Kinetic constants of the AtGH3.2 and AtGH3.6 enzymes for IAA, oxIAA, and Asp ($n = 3$). SD, standard deviation. (c) Model of IAA inactivation, adapted from Porco *et al.* (2016) and Hayashi *et al.* (2021), including the oxIAA-amino acid conjugation pathway mediated by GH3 enzymes identified in this study (red color). Dashed arrows indicate steps by yet-to-be-discovered enzymes.

that, unlike in angiosperms, the GH3-ILR1-DAO regulatory framework does not operate in nonflowering plants. The oxidative inactivation of IAA- and IAA-amino acid conjugates does not significantly maintain IAA homeostasis in spruce and is not mediated by DAO-like enzymes (Brunoni *et al.*, 2020; this study). The GH3-mediated IAA- and oxIAA-amino acid conjugation appear to be this species' primary auxin inactivation strategy (Brunoni *et al.*, 2020; this study). Distinctively, the metabolic fate of IAA and IAA metabolites is more similar between moss and Arabidopsis, as the oxidative pathway contributes the most to the metabolism of IAA-amino acid conjugates. The GH3-mediated conjugation of oxIAA to amino acids is a minor route in moss and Arabidopsis. Nonetheless, the GH3-ILR1-DAO pathway can unlikely regulate IAA metabolism in lower-land plants. DAO-like enzymes evolved specifically with angiosperms, ILL enzymes were not found in the moss *P. patens*, and the *Marchantia polymorpha* ILR1 is not employed in auxin conjugate hydrolysis in this liverwort (Campanella *et al.*, 2018, 2019; Brunoni *et al.*, 2020; Takehara *et al.*, 2020), suggesting that yet-to-be-discovered

enzymes could be responsible for oxidation and hydrolysis reactions in lower vascular plants. Altogether, the GH3-mediated oxIAA conjugation is a metabolic pathway that occurred early during plant evolution, and its contribution to IAA homeostasis is species-dependent.

Acknowledgements

This work was supported by the Ministry of Education, Youth and Sports of the Czech Republic (European Regional Development Fund-Project 'Plants as a tool for sustainable global development' no. CZ.02.1.01/0.0/0.0/16_019/0000827), by the Internal Grant of Palacký University Olomouc (IGA_PrF_2022_016) to ON, by the Czech Science Foundation (no. 21-07661S) to DK and by the Palacký University Olomouc Young Researcher grant (JG_2020_001) to MK, and (JG_2020_002) to AŽ. We thank Professor Jutta Ludwig-Müller for providing plasmids carrying *PpGH3.1* and *PpGH3.2* cds and Adam Klingberg (SkogForsk) for providing spruce seeds.

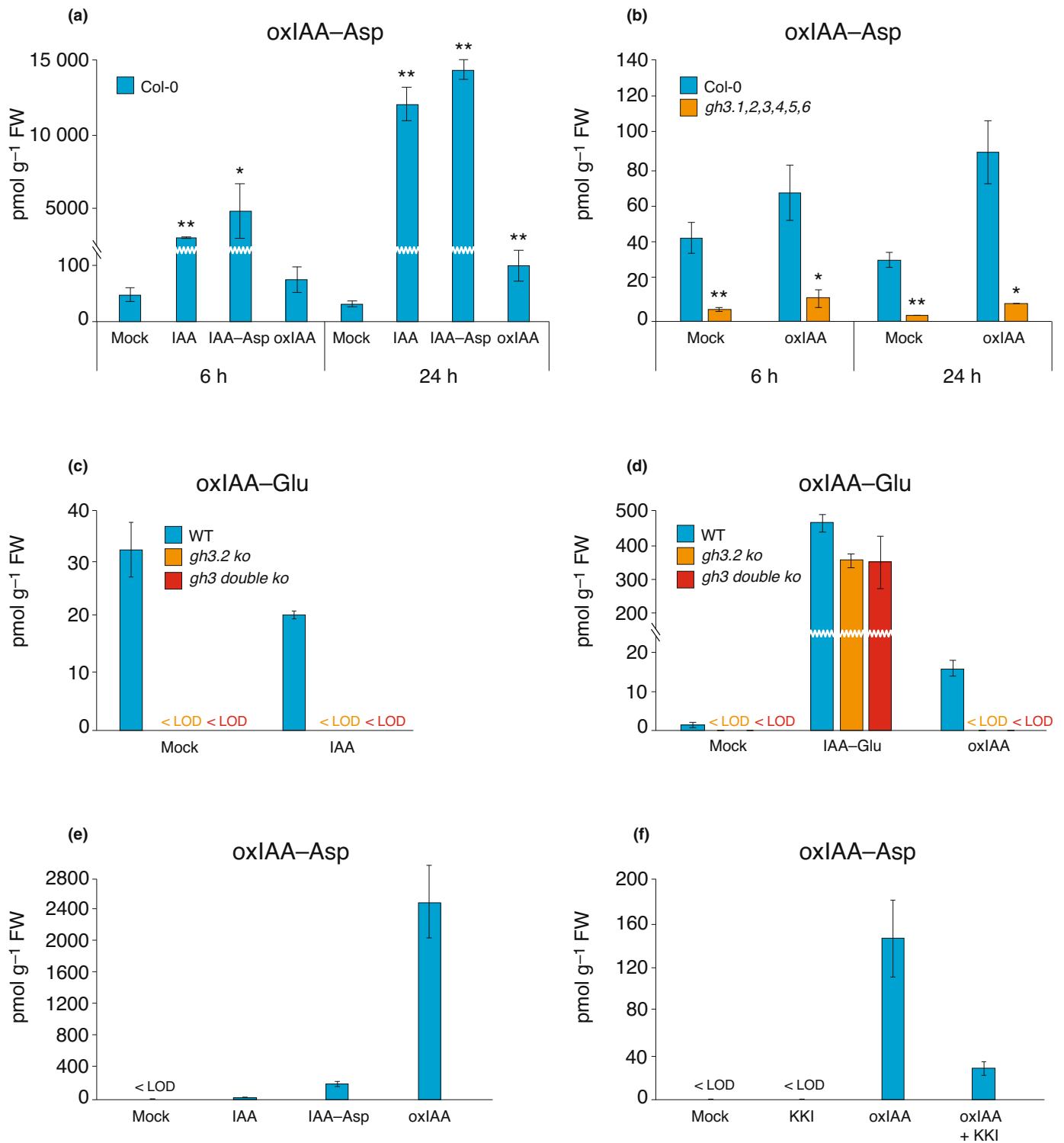


Fig. 2 Contribution of oxIAA-amino acid conjugation to auxin catabolism is species-dependent. (a, b) Formation of oxIAA-Asp after feeding of 7-d-after-germination *Arabidopsis* Col-0 with or without 50 μ M indole-3-acetic acid (IAA), IAA-Asp, and oxIAA for 6 and 24 h (a) and *gh3* sextuple mutant (*gh3.1*, *gh3.2*, *gh3.3*, *gh3.4*, *gh3.5*, and *gh3.6*) with or without 50 μ M oxIAA for 6 and 24 h (b). (c, d) Formation of oxIAA-Glu after feeding 3-wk-old *Physcomitrium patens* wild-type, *gh3.2* and *gh3.1 gh3.2* knockout mutant gametophores with or without 50 μ M IAA (c) and with or without 50 μ M IAA-Glu and oxIAA (d) for 24 h. (e, f) Formation of oxIAA-Asp after feeding 2-wk-old *Picea abies* seedlings with or without 50 μ M IAA, IAA-Asp, and oxIAA (e) and with or without 50 μ M KKI, 5 μ M oxIAA and KKI plus oxIAA (f) for 6 h. The concentrations are given in picomoles per gram fresh weight (FW). Samples were analyzed in three independent biological replicates, and error bars represent SD. Below the limit of detection, < LOD. Asterisks in (a, b) indicate statistically significant differences, as determined by Student's *t*-test: *, $P \leq 0.05$; **, $P \leq 0.01$.









Competing interests









None declared.

Author contributions

FB and ON conceived the experiments. FB, AP, AŽ, SC and DK designed the experiments. FB, AP, AŽ, AA and MK performed the experiments. FB wrote the paper with input from all the authors.

ORCID

Anita Ament  <https://orcid.org/0000-0001-5563-7330>
 Federica Brunoni  <https://orcid.org/0000-0003-1497-9419>
 Silvio Collani  <https://orcid.org/0000-0002-9603-0882>
 Martina Kopečná  <https://orcid.org/0000-0003-2136-4615>
 David Kopečný  <https://orcid.org/0000-0002-4309-4284>
 Ondřej Novák  <https://orcid.org/0000-0003-3452-0154>
 Aleš Pěničák  <https://orcid.org/0000-0002-1314-2249>
 Asta Žukauskaitė  <https://orcid.org/0000-0001-6759-8789>

Federica Brunoni^{1*} , **Aleš Pěničák**¹ ,
Asta Žukauskaitė² , **Anita Ament**¹ ,
Martina Kopečná³ , **Silvio Collani**⁴ ,
David Kopečný³  and **Ondřej Novák**^{1*} 

¹Laboratory of Growth Regulators, Institute of Experimental Botany of the Czech Academy of Sciences, Faculty of Science of Palacký University, Olomouc CZ-78371, Czech Republic;

²Department of Chemical Biology, Faculty of Science, Palacký University, Olomouc CZ-78371, Czech Republic;

³Department of Experimental Biology, Faculty of Science, Palacký University, Olomouc CZ-78371, Czech Republic;

⁴Department of Plant Physiology, Umeå Plant Science Centre, Umeå University, Umeå SE-90736, Sweden

(*Authors for correspondence: emails federica.brunoni@upol.cz; novako@ueb.cas.cz)

References

- Bierfreund NM, Tintelnot S, Reski R, Decker EL. 2004. Loss of *GH3* function does not affect phytochrome-mediated development in a moss, *Physcomitrella patens*. *Journal of Plant Physiology* 161: 823–835.
- Brunoni F, Collani S, Casanova-Sáez R, Šimura J, Karady M, Schmid M, Ljung K, Bellini C. 2020. Conifers exhibit a characteristic inactivation of auxin to maintain tissue homeostasis. *New Phytologist* 226: 1753–1765.
- Brunoni F, Collani S, Šimura J, Schmid M, Bellini C, Ljung K. 2019. A bacterial assay for rapid screening of IAA catabolic enzymes. *Plant Methods* 15: 126.
- Campanella JJ, Kurdach S, Bochis J, Smalley JV. 2018. Evidence for exaptation of the *Marchantia polymorpha* M20D peptidase MpILR1 into the tracheophyte auxin regulatory pathway. *Plant Physiology* 177: 1595–1604.
- Campanella JJ, Kurdach S, Skibitski R, Smalley JV, Desind S, Ludwig-Müller J. 2019. Evidence for the early evolutionary loss of the M20D auxin amidohydrolase family from mosses and horizontal gene transfer from soil bacteria of cryptic hydrolase orthologues to *Physcomitrella patens*. *Journal of Plant Growth Regulation* 38: 1428–1438.
- Delfin JC, Kanno Y, Seo M, Kitaoka N, Matsuura H, Tohge T, Shimizu T. 2022. AtGH3.10 is another jasmonic acid-amido synthetase in *Arabidopsis thaliana*. *The Plant Journal* 110: 1082–1096.
- Friml J. 2022. Fourteen stations of auxin. *Cold Spring Harbor Perspectives in Biology* 14: a039859.
- Fukui K, Arai K, Tanaka Y, Aoi Y, Kukshal V, Jez JM, Kubeš M, Napier R, Zhao Y, Kasahara H *et al.* 2022. Chemical inhibition of the auxin inactivation pathway uncovers the roles of metabolic turnover in auxin homeostasis. *Proceedings of the National Academy of Sciences, USA* 119: e2206869119.
- Hayashi KI, Arai K, Aoi Y, Tanaka Y, Hira H, Guo R, Hu Y, Chennan G, Zhao Y, Kasahara H *et al.* 2021. The main oxidative inactivation pathway of the plant hormone auxin. *Nature Communications* 12: 6752.
- Holland CK, Westfall CS, Schaffer JE, De Santiago A, Zubieta C, Alvarez S, Jez JM. 2019. *Brassicaceae*-specific Gretchen Hagen 3 acyl acid amido synthetases conjugate amino acids to chorismate, a precursor of aromatic amino acids and salicylic acid. *Journal of Biological Chemistry* 294: 16855–16864.
- Kaneko S, Cook SD, Aoi Y, Watanabe A, Hayashi KI, Kasahara H. 2020. An evolutionarily primitive and distinct auxin metabolism in the lycophyte *Selaginella moellendorffii*. *Plant and Cell Physiology* 61: 1724–1732.
- LeClere S, Tellez R, Rampey RA, Matsuda SP, Bartel B. 2002. Characterization of a family of IAA-amino acid conjugate hydrolases from *Arabidopsis*. *Journal of Biological Chemistry* 277: 20446–20452.
- Ludwig-Müller J, Jülke S, Bierfreund NM, Decker EL, Reski R. 2009. Moss (*Physcomitrella patens*) GH3 proteins act in auxin homeostasis. *New Phytologist* 181: 323–338.
- Müller K, Dobrev PI, Pěničák A, Hošek P, Vondráková Z, Filepová R, Malínská K, Brunoni F, Helusová L, Moravec T *et al.* 2021. DIOXYGENASE FOR AUXIN OXIDATION 1 catalyzes the oxidation of IAA amino acid conjugates. *Plant Physiology* 187: 103–115.
- Okrent RA, Brooks MD, Wildermuth MC. 2009. *Arabidopsis* GH3.12 (PBS3) conjugates amino acids to 4-substituted benzoates and is inhibited by salicylate. *Journal of Biological Chemistry* 284: 9742–9754.
- Okrent RA, Wildermuth MC. 2011. Evolutionary history of the GH3 family of acyl adenylases in rosids. *Plant Molecular Biology* 76: 489–505.
- Pěničák A, Casanova-Sáez R, Pilařová V, Žukauskaitė A, Pinto R, Micol JL, Ljung K, Novák O. 2018. Ultra-rapid auxin metabolite profiling for high-throughput mutant screening in *Arabidopsis*. *Journal of Experimental Botany* 69: 2569–2579.
- Porco S, Pěničák A, Rashed A, Voß U, Casanova-Sáez R, Bishopp A, Bishopp A, Golebiowska A, Bhosale R, Swarup R *et al.* 2016. Dioxygenase-encoding *AtDAO1* gene controls IAA oxidation and homeostasis in *Arabidopsis*. *Proceedings of the National Academy of Sciences, USA* 113: 11016–11021.
- Ross JJ, Gélinas-Marion A. 2021. Two pathways become one. *Nature Plants* 7: 1546–1547.
- Staswick PE, Serban B, Rowe M, Tiriyaki I, Maldonado MT, Maldonado MC, Suza W. 2005. Characterization of an *Arabidopsis* enzyme family that conjugates amino acids to indole-3-acetic acid. *Plant Cell* 17: 616–627.
- Staswick PE, Tiriyaki I. 2004. The oxylipin signal jasmonic acid is activated by an enzyme that conjugates it to isoleucine in *Arabidopsis*. *Plant Cell* 16: 2117–2127.
- Takehara S, Sakuraba S, Mikami B, Yoshida H, Yoshimura H, Itoh A, Endo M, Watanabe N, Nagae T, Matsuoka M *et al.* 2020. A common allosteric mechanism regulates homeostatic inactivation of auxin and gibberellin. *Nature Communications* 11: 2143.
- Torrens-Spence MP, Bobokalonova A, Carballo V, Glinkerman CM, Pluskal T, Shen A, Weng JK. 2019. PBS3 and EPS1 complete salicylic acid biosynthesis from isochorismate in *Arabidopsis*. *Molecular Plant* 12: 1577–1586.
- Westfall CS, Zubieta C, Herrmann J, Kapp U, Nanao MH, Jez JM. 2012. Structural basis for pre-receptor modulation of plant hormones by GH3 proteins. *Science* 336: 1708–1711.
- Zhang J, Lin JE, Harris C, Campos Mastrotti Pereira F, Wu F, Blakeslee JJ, Peer WA. 2016. DAO1 catalyzes temporal and tissue-specific oxidative inactivation of auxin in *Arabidopsis thaliana*. *Proceedings of the National Academy of Sciences, USA* 113: 11010–11015.

Supporting Information

Additional Supporting Information may be found online in the Supporting Information section at the end of the article.

Dataset S1 Raw mass spectrometry data of indole-3-acetic acid (IAA)- and oxIAA-amino acid conjugates from the bacterial assay.

Dataset S2 Raw mass spectrometry data of indole-3-acetic acid metabolites from *in vitro* enzymatic activity and *in planta*-feeding assays.

Fig. S1 Bacterial assay of oxIAA conjugation by recombinant *Arabidopsis* GRETCHEN HAGEN 3s.

Fig. S2 Levels of oxIAA–Glu in *Arabidopsis* Col-0 and *gh3* sextuple mutant after feeding with indole-3-acetic acid (IAA) metabolites.

Fig. S3 Bacterial assay of oxIAA conjugation by recombinant moss GRETCHEN HAGEN 3.

Fig. S4 Bacterial assay of oxIAA conjugation by recombinant spruce GRETCHEN HAGEN 3s.

Fig. S5 Levels of oxIAA–Glu in spruce seedlings after feeding with indole-3-acetic acid (IAA) metabolites and the GRETCHEN HAGEN 3 inhibitor KKI.

Table S1 List of primers used for cloning in this work.

Please note: Wiley is not responsible for the content or functionality of any Supporting Information supplied by the authors. Any queries (other than missing material) should be directed to the *New Phytologist* Central Office.

Key words: *Arabidopsis*, auxin inactivation, conjugation, moss, oxidation, spruce.

Received, 3 December 2022; accepted, 11 March 2023.